Intense wind-driven coastal upwelling in the Balearic Islands in response to storm Blas (November 2021)

Baptiste Mourre[1], Emma Reyes[1], Pablo Lorente[2], Alex Santana[1], Jaime Hernández-Lasheras[1], Ismael Hernández-Carrasco[1], Maximo García-Jove[1], Nikolaos D. Zarokanellos[1]

[1]SOCIB, Balearic Islands Coastal Observing and Forecasting System, Palma, 07122, Spain
[2]Puertos del Estado, Madrid, 28042, Spain

Correspondence to: Baptiste Mourre (bmourre@socib.es)

Abstract.

This article analyzes the Balearic Islands wind-driven coastal upwelling in response to the intense and long-lasting storm Blas which affected the Western Mediterranean Sea in November 2021. The storm was associated with a pronounced pressure low, generating heavy rains and intense winds and showing some characteristics of a tropical cyclone. The Balearic Islands area was particularly affected since the core of the storm was moving over a one-week-long period from the south-west of this area to just above Menorca and Mallorca Islands. High-resolution regional forecast models indicated that the intense northeasterly winds blowing over the region during the first days of the storm led to the development of intense upwellings along the northwestern coasts of Mallorca and Ibiza Islands together with a reversal of the surface current. While the clouds associated with the storm prevented the radiometers onboard satellites to precisely observe the evolution of the sea surface signature of the upwelling, signals of enhanced chlorophyll concentration were still detected in the upwelling region. The high-resolution Western Mediterranean Operational model, which downscales the Copernicus Marine Service Mediterranean predictions, is used to describe the characteristics of this intense coastal upwelling event, as well as to analyze its singularity over the past 9-year time series through the comparison of different coastal upwelling indices. The upwelling event is found to have a duration of three days (considering its effects on the sea surface temperature) with a spatial off-shore extension of around 20km. It was characterized by intense cold coastal sea surface anomalies of around 6ºC. While it was the most intense event over the past 9 years in terms of local cross-shore sea surface temperature gradients, it is ranked second in terms of the intensity of cross-shelf transports, behind storm Gloria upwelling event in January 2020. This study demonstrates the benefits of operational oceanography for the characterization of extreme events through the provision of time series of high-resolution modelling results in the coastal area.

Short summary

We characterize the surface and vertical signature of an intense storm-induced coastal upwelling along the northwestern coast of the Balearic Islands in 2021, using a high-resolution operational prediction model. The upwelling, with a duration around three days and a spatial off-shore extension of 20km, led to cross-shore surface temperature differences of up to 6ºC. It was the most intense event of the past 9 years in terms of the impact on temperature, and the second one in terms of cross-shore transports.

1- Introduction

Storm Blas[1] was an intense Mediterranean cyclone which affected the Western Mediterranean Sea from 6 to 18 November 2021. It was first identified on 6 November between the Balearic Islands and Sardinia before moving westwards towards the Balearic archipelago. After the core of the storm looped over Mallorca Island on 11 November, exhibiting a well-defined circular deep (~10hPa) low-pressure center, it then moved eastwards while developing a spiral structure resembling that of tropical cyclones. The storm then moved over Sardinia and Corsica Islands before weakening and dissipating in the Tyrrhenian Sea on 18 November. Panels a and b in Figure 1 show the distribution of clouds over the affected area on 7 and 13 November as observed by Sentinel-3 Ocean and Land Color Instrument (OLCI) satellite true color images.

This situation created extreme conditions of intense winds and high waves as well as heavy rainfall in the Balearic archipelago. In particular, intense northeasterly winds were blowing over the area during the first phase of the storm from 5 to 7 November (Figure 1 panels c,d), creating favorable conditions for coastal upwelling along the northwestern coasts of Mallorca and Ibiza Islands. The peak of this wind event occurred on 6 November around 10:00 UTC, with hourly mean values over 17.5 m/s off Mallorca Island as represented by the HARMONIE-AROME model (Bengtsson et al., 2017) from the Spanish Meteorological Agency (AEMET).

Coastal upwelling is an oceanic process which generates upward vertical currents at the coast in response to an offshore transport of surface waters produced under the action of an intense or sustained alongshore wind stress. In the northern hemisphere, the wind has to blow with the coast on its left-hand-side to be favorable to upwelling. By bringing cold and nutrient-rich deep waters close to the surface, the upwelling has significant effects on the physical and biogeochemical characteristics of coastal waters, generally enhancing the local primary productivity and then playing an important role on marine ecosystems (Pauly and Christensen, 1995). In the Western Mediterranean Sea, wind-induced upwelling is known to occur along the French coast (Millot et al, 1979, Ray et al. 2000, Bakun and Agostini, 2001), western and eastern coasts of Sardinia (Olita et al, 2013, Salusti et al., 1998) and northwestern Alboran Sea (Sarhan et al., 2000, Macias et al., 2008). Eddy-induced coastal upwelling has also been evidenced in the Ligurian Sea (Casella et al., 2011) and along the Algerian coast (Millot et al., 1985). To our knowledge, no upwelling has yet been reported in the Balearic Islands. While the frequent north-

[1] https://www.aemet.es/en/conocermas/borrascas/2021-2022/estudios_e_impactos/blas

northwesterly mistral wind events do not present the appropriate orientation to generate upwelling along the northwestern coast of the Balearic Islands, favorable conditions with intense northeasterly winds are occasionally met during specific storms such as Gloria in January 2020 (Amores et al., 2020, Sotillo et al., 2021, Álvarez-Fanjul et al. 2022) or Blas in November 2021. Notice that these winds blow in the opposite direction of the established Balearic Current, which flows northeastwards along the northwestern coast of the Balearic Islands (Lopez-García et al., 1994).

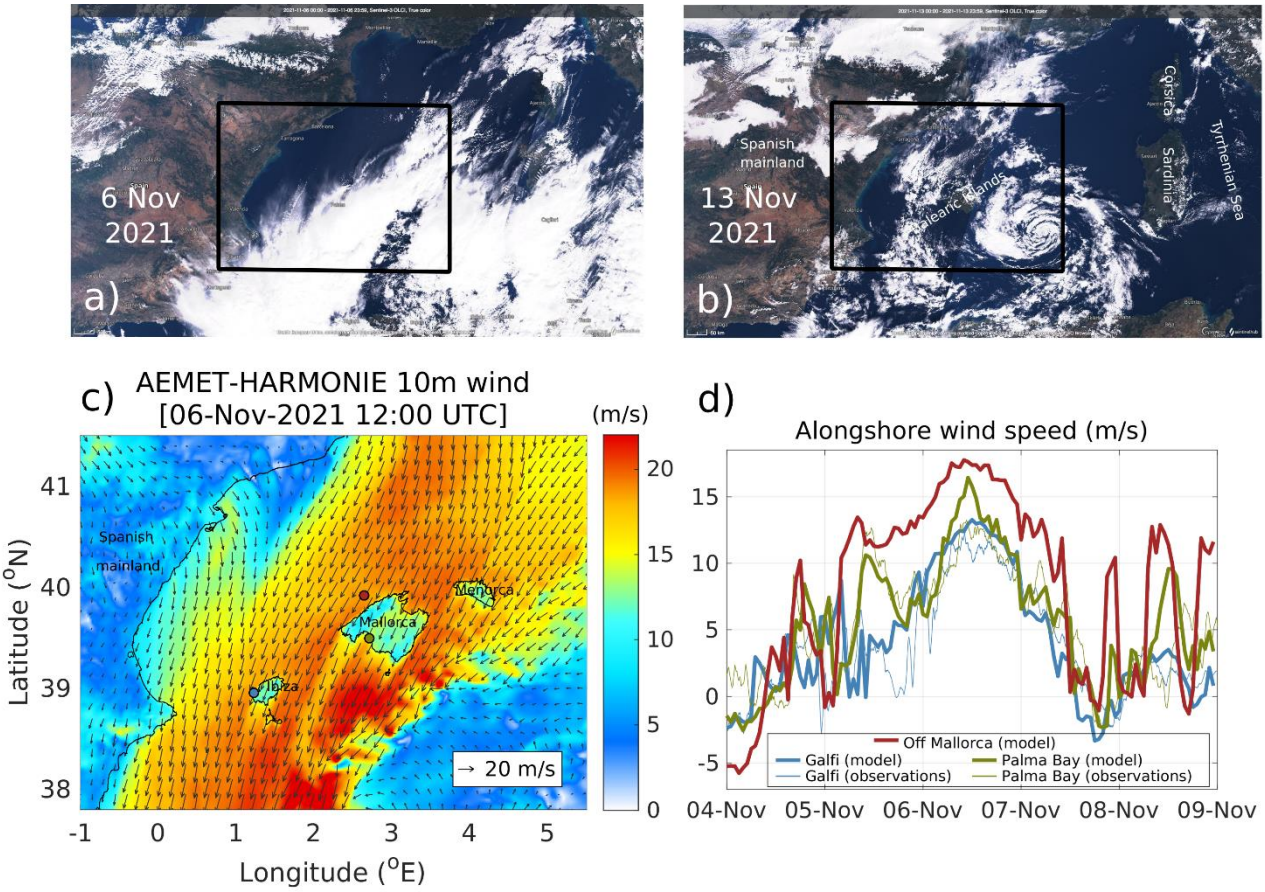

Figure 1: Upper panels: True color image from Sentinel-3 OLCI captured over the Western Mediterranean Sea on a) 6 November 2021 and b) 13 November 2021. Lower panels: c) 10m wind map on 6 November 2021 from the AEMET HARMONIE-AROME prediction model over the area delimited by the black rectangles in panels a) and b); and d) time series of alongshore 10m wind speed from model and observations at the three locations (1-Automatic Weather Station of Puig des Galfí in Ibiza, 2- Oceanographic buoy of Palma Bay in Mallorca, and 3- virtual station off the northwestern coast of Mallorca) represented in panel c). "Alongshore" is here defined considering the direction of the northwestern coast of Mallorca Island making an angle of 123º with respect to the North, with positive values southwestwards.

This study was motivated by the intense sea surface temperature (SST) gradients along the northwestern coast of the Balearic Islands seen in high-resolution regional prediction models during the first phase of storm Blas, together with observations of surface current reversal from High-Frequency (HF) radar measurements along the northwestern coast of Ibiza Island. The objective of this study is to characterize this unusually intense upwelling in terms of both its surface signature and its vertical structure, as well as to evaluate its singularity within the time series of different upwelling indices computed over the past

decade. The main source of information is a high-resolution numerical prediction model given the very limited number of in-situ and satellite observations available during this event.

2- Data and methods

2.1 Numerical models

We analyze the outputs of the Western Mediterranean Operational prediction system (WMOP[2], Juza et al., 2016; Mourre et al., 2018) developed at the Balearic Islands Coastal Observing and Forecasting System (SOCIB, Tintoré et al., 2013). WMOP is a 2-km regional configuration of the ROMS modelling system (Shchepetkin and McWilliams, 2005) implemented over the Western Mediterranean Sea. It uses high-resolution (1h, 2.5km) atmospheric forcing from the HARMONIE-AROME model (Bengtsson et al., 2017) provided by AEMET. Notice that before February 2019, the HIRLAM model was used as atmospheric forcing with a resolution of 5km and 1h (3h before March 2017). WMOP downscales the conditions of the Copernicus Marine Service Mediterranean analysis and forecast model (CMEMS-MED, Clementi et al., 2021), which are used as open boundary conditions. It also includes assimilation of observations from satellite SST, along-track sea level anomaly, Argo temperature and salinity profiles as well as surface currents in the Ibiza channel applying a local multimodel Ensemble Optimal Interpolation approach as described in Hernández-Lasheras and Mourre (2018) and Hernández-Lasheras et al. (2022), with a 3-day cycle.

We also consider the outputs of the CMEMS-MED model, which provides a spatial resolution of around 4km. This system includes variational data assimilation of temperature and salinity vertical profiles and along track satellite Sea Level Anomaly observations through a 3DVAR scheme (Dobricic and Pinardi, 2008). The atmospheric forcing is provided by the predictions from the European Center for Medium-Range Weather Forecasts[3] with a spatial resolution close to 10km and a temporal resolution of 1h.

2.2 Ocean color satellite observations

High resolution ocean color imagery was analyzed to detect the enhancement of the surface chlorophyll-a (Chla) concentration during the upwelling. The Level-3 ocean color product distributed by the Copernicus Marine Service (Volpe et al. 2019) was used. It provides surface Chla concentration from the OLCI Instrument onboard the Sentinel-3 satellite with a 300m-resolution. Notice that clouds were present over the study area during the storm period, which limited the availability of exploitable high-

[2] https://www.socib.es/?seccion=modelling&facility=forecast
[3] https://www.ecmwf.int

resolution satellite observations. The Sentinel3-OLCI observations were the only available satellite data that were found to give relevant information for the detection of the upwelling signature during the study period.

2.3 Upwelling indices

Several upwelling indices (UIs) have been used in the literature with the objective to estimate the intensity of coastal upwelling. These indices are based on either the cross-shore SST differences (Demarcq and Faure, 2000), the along-shore surface current velocities (Lorente et al., 2020) or the cross-shore Ekman transport related to the forcing winds (Bakun, 1973), sometimes also incorporating the effect of cross-shore geostrophic flows (Marchesiello and Estrade, 2010; Rossi et al., 2013, Jacox et al., 2018) , or. This study compares four UIs computed over the 9-year time series of the WMOP operational model outputs:

(i) UI_{SST} first quantifies the temperature differences between the coast (SST_{coast}) and a location 25km offshore ($SST_{offshore}$) off the northwestern coast of Mallorca Island (edges of the magenta cross-shore section illustrated in Figure 2a). As in Marchesiello and Estrade (2010), the observed differences are normalized by the vertical temperature differences between the surface and 200m depth (T^{200m}) at the offshore end of the section according to the following formula:

$$UI_{SST} = \frac{SST_{offshore} - SST_{coast}}{SST_{offshore} - T^{200m}{}_{offshore}} \quad (1)$$

This normalized formulation allows to scale the horizontal temperature differences by the vertical ones. A value close to one indicates a fully developed upwelling with SST values at the coast equal to the temperatures at 200m depth. Since this formulation of UI_{SST} generates very high values in situations when the upper ocean is vertically mixed during winter (denominator close to zero), the index is only computed here when the vertical temperature difference is larger than 1ºC.

(ii) The second index is based on alongshore surface current velocities, as first proposed in Lorente et al. (2020) as a proof-of-concept investigation. This index was specifically designed to be applied in any coastal area where surface velocities are available from HF radar instruments. It assumes that the alongshore wind stress is the primary driver of upwelling circulation and that the surface currents are highly responsive to local winds (e.g. Paduan and Ronsenfeld, 1996; Kohut et al., 2006). This index is defined here as the average alongshore surface velocity ($V^{surf}{}_{alongshore}$) in the 25km-wide coastal region off the northwestern coast of Mallorca Island, following Eq 2.

$$UI_{alongshore\ velocity} = \overline{V^{surf}{}_{alongshore}} \quad (2)$$

The overbar denotes the average over the rectangular box containing the two magenta sections represented in Figure 2. The alongshore direction is the direction of the corresponding magenta section. It makes an angle of 123º with respect to the North. Positive values denote southwestwards flows. Further details about the methodology and application of this index can be found in Lorente et al. (2022, present issue of the Ocean State Report).

(iii) The third index is the classical cross-shore Ekman transport index, computed from the alongshore wind stress. It is defined as follows:

$$UI_{Ekman\ transport} = \int_{x=0}^{x=L} \frac{\tau_{alongshore}}{\rho\, f}\, dx \qquad (3)$$

where $\tau_{alongshore}$ is the alongshore wind stress, ρ is the water density and f the Coriolis frequency. The integral is computed along the magenta alongshore section over a distance L of 60km. $UI_{Ekman\ transport}$ represents the total transport across this section. Positive values indicate an offshore transport.

(iv) Finally, the last index computes the total cross-shore model transport in the upper 50m across the same section. This depth approximately corresponds to the depth of the Ekman layer as illustrated in Figure 3. It does not only include the Ekman transport, but also the cross-shore geostrophic transport and other contributions due to the cross-shore wind component and potential effects associated with the spatial variability of the wind stress curl. It is calculated following Eq. (4):

$$UI_{total\ transport} = \int_{z=0}^{z=50m} \int_{x=0}^{x=L} V_{cross-shore}\, dx\, dz \qquad (4)$$

where $V_{cross\text{-}shore}$ is the model horizontal velocity in the cross-shore direction.

3- Surface expression of the upwelling

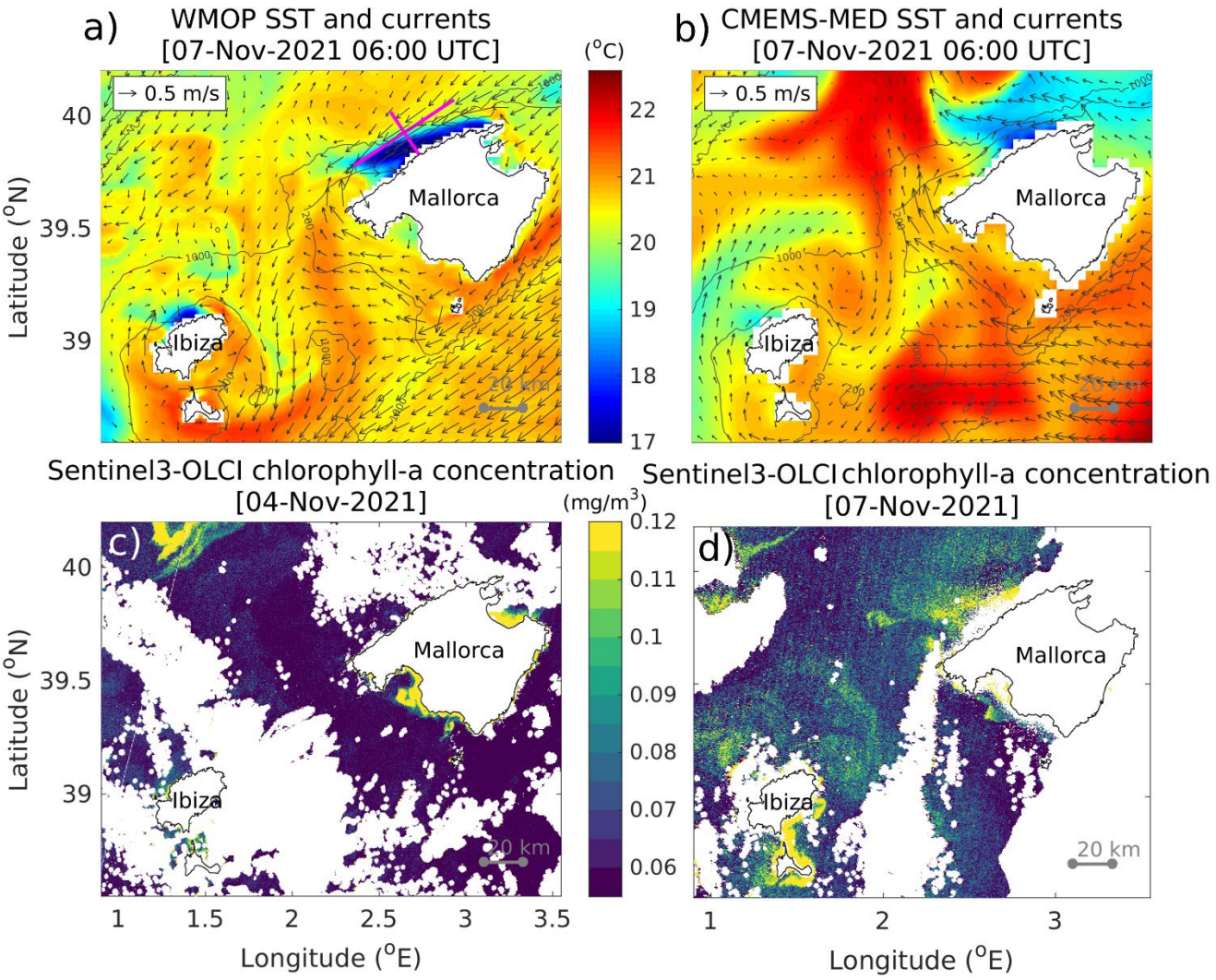

Figure 2: Upper panels: SST and surface currents around Mallorca and Ibiza Islands on 7 November 2021 at 06:00 UTC as represented by a) WMOP and b) CMEMS-MED models. In panel a), the lines in magenta represent the alongshore and cross-shore sections used in Sections 3 and 4. Lower panels: chlorophyll-a concentration as observed by Sentinel3-OLCI on c) 4 November and d) 7 November (i.e. before and during storm Blas, respectively).

Figure 2 illustrates the surface circulation patterns and associated SST in the WMOP and CMEMS-MED predictions models on 7 November 2022 at 06:00 UTC (the time with the most significant impact of the upwelling on the SST). The SST exhibits marked upwelling signatures in the WMOP model along the northwestern coast of Mallorca and Ibiza Islands, with the temperature of surface waters around 6ºC colder at the coast compared to 20km offshore. The surface coastal current flows southwestwards along the wind direction, which is reversed with respect to the direction of the Balearic Current under normal

conditions (Lopez-García et al., 1994). The offshore width of the upwelled water region ranges from 10 to 20km, which slightly extends off the 200m isobath. The upwelling is also represented in the CMEMS-MED model, but with a less pronounced signature. It is out of the scope of this short article to investigate these differences between models, but the lower spatial resolution of both the model grid and atmospheric forcing may have an important role in producing these discrepancies. The upwelled water only reaches the surface in the northern half of the northwestern coast of Mallorca Island in CMEMS-MED, yet with a larger offshore extension compared to WMOP. The event duration based on its effect on the SST was around three days, i.e. from 5 November at 15:00 UTC when the first cross-shore coastal SST gradients were observed until 8 November at 12:00 UTC when they vanished.

As illustrated in Figure 1, the storm was associated with a dense cloud coverage, which only allowed very partial satellite remote sensing information on SST and Chla concentration. Despite this important limitation, the two most relevant ocean color images illustrated in Figure 2 hint at the enhancement of the Chla concentration along the northwestern coast of Mallorca Island. While a low concentration of Chla was detected on 4 November before the storm, a significant increase was observed on 7 November. The Chla concentration reached 0.1 mg/m3, a magnitude more than twice larger than that observed 3 days before. While the satellite-derived Chla in coastal areas should be interpreted carefully, particularly under cloudy conditions, no evident errors have been identified in the associated Quality Index (QI). QI measures for every pixel the difference between the observation and the climatological average, normalized by the climatological standard deviation. The QI maps for 4 and 7 November are included in the supplementary material (Figure R1), showing values ranging from 1 to 2 in the area of enhanced Chla, with a peak above 4 in the near-coastal zone. Moreover, sediment resuspension is unlikely to affect the quality of the data due to the steep local topography. Also, the Lagrangian analysis of surface water trajectories in the northern part of Mallorca Island (Figure R2 provided in the supplementary material) allows to reject the hypothesis of a lateral advection of Chla from the northern bay (Alcudia Bay) towards the northwestern coast of the island. As a consequence, and within the limitations of both the model and observations, we believe that the spatial consistency between the observed patch of enhanced Chla and the model upwelling area is probably indicative of an upwelling-induced local enhancement of Chla.

3- Vertical structure

Figure 3 illustrates the vertical structure of the temperature and velocity fields along the cross-shore section off the northwestern coast of Mallorca Island, as represented by the WMOP model. While velocities are illustrated on 6 November at 12:00 UTC, corresponding to the maximum wind intensity in this area (Figure 1), the temperature is displayed 18 hours later to illustrate the time with the maximum signature in SST. The temperature section (Figure 3a) shows a typical pattern of upwelling with an upward tilting of the isotherms towards the coast, which is associated with an upward transport of colder deep waters along the topographic slope. The surface temperature decreases by 6ºC across the upwelling front, varying from 20.6ºC 20km offshore, where the mixed layer depth is around 50m, to 14.6ºC at the coast. The cross-shore velocity section (Figure 3b) shows an offshore displacement of surface waters in the upper 50m, consistent with the Ekman theory in the

presence of alongshore winds. Cross-shore velocities (Figure 3c) reach 0.3 m/s. The alongshore velocity along this cross-shelf section is characterized by the intense southwestward coastal jet with surface velocities exceeding 1m/s. Upward vertical velocities (Figure 3d) are enhanced along the topographic slope, with values between 40 and 60m/day in the upper 100m and in the first 12km from the coast. Overall, these cross-shelf sections illustrate a relatively thin (cross-shore extension around 20km) but intense upwelling with a significant coastal jet.

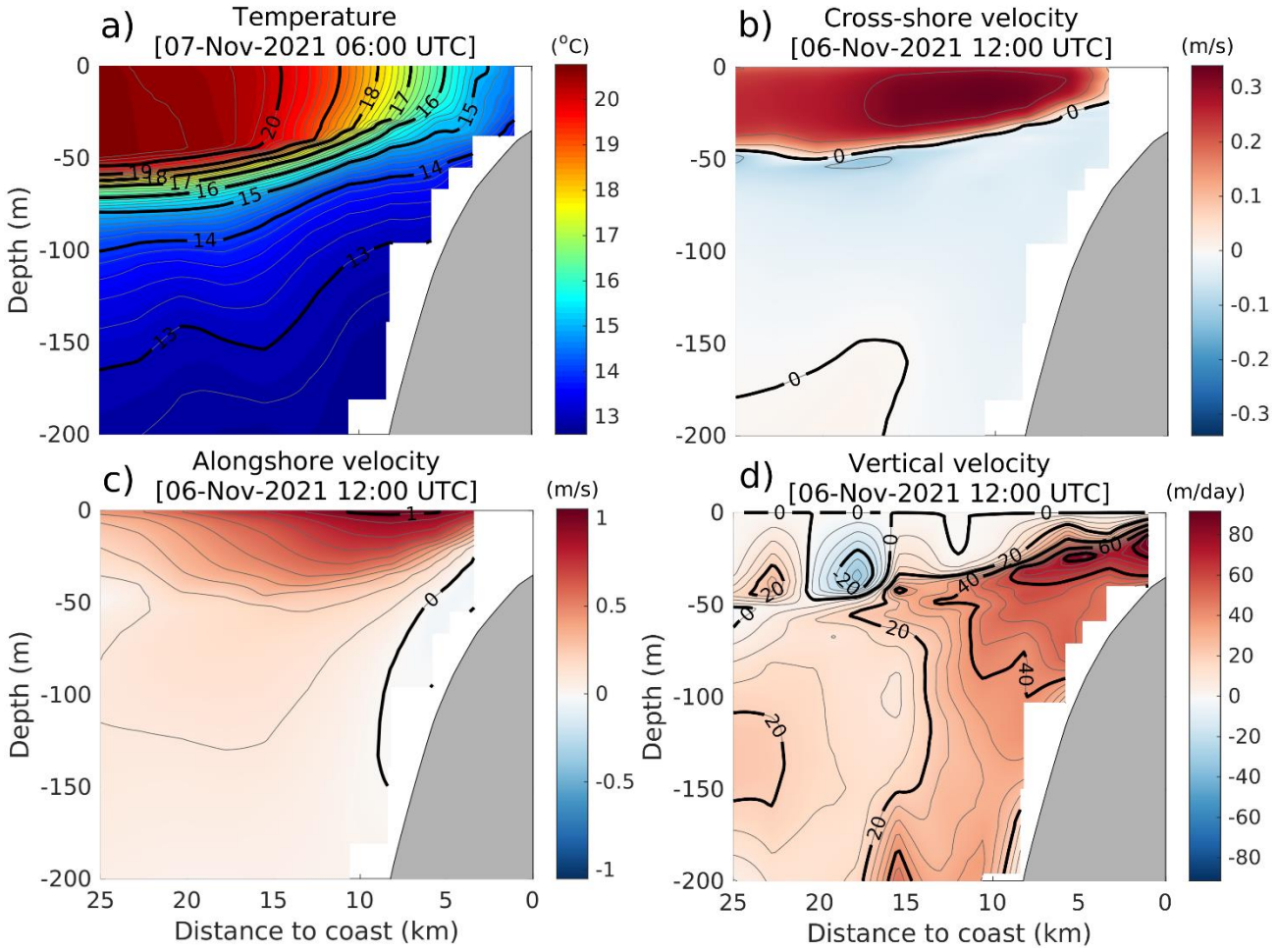

Figure 3: Sections of WMOP model fields along the cross-shore magenta line represented in Figure 2: a) temperature on 7 November 2021 at 06:00 UTC, b) cross-shore velocity, c) alongshore velocity and d) vertical velocity on 6 November 2021 at 12:00 UTC.

4- Interannual perspective

How singular was this intense wind-driven coastal upwelling event? To answer this question, we compute here several upwelling indices (described in section 2.3) over the whole WMOP model time series covering the 9-year period between August 2013 and June 2022. The first index, representing the normalized cross-shelf SST gradients, ranks the November 2021 event (i.e. Blas storm) as the most intense event of the whole time series. It is the only event with a normalized cross-shelf SST gradient exceeding 0.5. The event is also the most intense according to the second index which measures the intensity of the alongshore surface velocity. However, the Ekman and total cross-shelf transport indices indicate a larger transport during the other extreme event associated with storm Gloria in January 2020. This is especially true for the total transport which also accounts for the effects of the wind stress curl and cross-shore geostrophic transport. During both Gloria and Blas upwelling events, the offshore total transport was enhanced with respect to the Ekman estimate. A third very intense storm in January 2017 (also documented in García-León et al., 2018) led to a slightly larger cross-shore Ekman transport but a lower total transport compared to Blas. The effects on the SST and coastal jet are particularly marked during the Blas upwelling event due to its occurrence in early November when the surface ocean stratification was still significant. On the contrary and despite the intense offshore transport during the upwelling event associated with storm Gloria, the effects on the SST were hardly noticeable due to the presence of mixed surface waters. Let´s remind here that the SST index is only computed when the vertical temperature difference between the surface and 200m depth is larger than 1ºC, which significantly limits the use of the SST-based index during the winter season. However, this was not the case during the Gloria event, which showed values just above 1ºC.

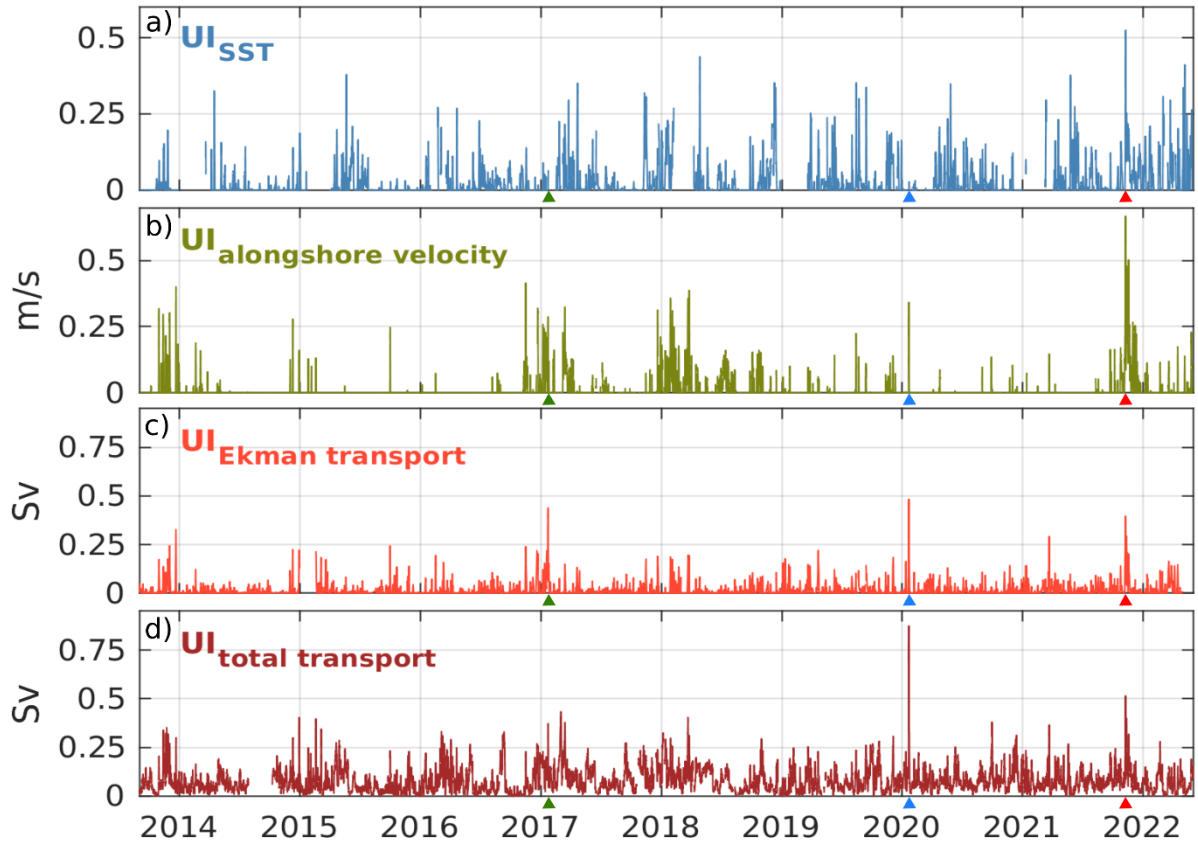

Figure 4: Time series of upwelling indices defined in Section 2.3 between August 2013 and June 2022 (3-hourly values are shown after applying a 24-hour running average): a) cross-shore normalized SST gradient index, b) alongshore velocity index, c) cross-shore Ekman transport index, d) cross-shore total transport index. The red, blue and green triangles on the x-axis mark the time of Blas, Gloria and January 2017 storms, respectively.

5- Conclusions

This study describes some of the characteristics of a short (5-8 November 2021) but intense wind-driven coastal upwelling event along the northwestern coast of the Balearic Islands as represented by a high-resolution forecast model during storm Blas in November 2021. The time series of several upwelling indices illustrate the episodicity of upwelling events in this area, mainly related to their nature related to the occurrence of storms with intense northeasterly winds.

While the November 2021 Blas-related event was the most intense in terms of the effects on the SST and alongshore velocities over the 9-year-long analyzed time series, the induced cross-shelf surface transport was lower than that modelled during storm Gloria in January 2020, whose effects on the wind, waves, sea level and currents were already reported as a record-breaking

event in the literature (Álvarez-Fanjul et al. 2022). This comparison illustrates the difference between upwelling indices for the characterization of the intensity of these events. In particular, the magnitude of SST gradients or alongshore velocity does not necessarily reveal the whole intensity of the underlying offshore transport. A careful analysis of the time series would allow to determine appropriate thresholds for the different indices so as to define suitable criteria for the identification of the upwelling. The duration would certainly be an additional relevant parameter for the operational definition of these events. Here, for instance, the event duration corresponding to a threshold of 0.25Sv for the total offshore transport was 42 hours for the Blas-related upwelling, 51 hours for Gloria and 21 hours for the January 2017 event. In the particular case of Blas, this duration is shorter than 3 days, i.e. the value obtained when considering the effect on the SST, highlighting the sensitivity of these metrics to the index and threshold under consideration.

Such storm-driven coastal upwelling is especially difficult to monitor given their short time scale and the absence of in situ observations in this area. The dense cloud coverage associated with the storm also significantly limits the availability of high-resolution satellite observations to characterize the surface signature of the phenomenon. In this context, high-resolution operational regional ocean models help overcome these limitations providing timely and accurate information to identify and characterize these events. The only available ocean color image from satellite suggests an increase in primary productivity in a coastal area which corresponds to the area of upwelled water in the model. While the lack of complementary observations prevents from properly evaluating the realism of the model fields, the consistency between the spatial structure of observed Chla enhancement and model upwelled water seems to indicate a reasonable representation of the effect of the upwelling process in the model. High spatial resolution (close to kilometric) is needed in both the model grid and the atmospheric forcing to describe such coastal phenomena whose cross-shore extension does not exceed 20km.

Despite its short duration, this phenomenon was found to be sufficient to enhance the surface Chla concentration. A more comprehensive understanding of the impacts of these storm-related upwelling events on local ecosystems would need further investigation requiring dedicated monitoring systems. Underwater gliders equipped with sensors of both physical and biogeochemical parameters can be suitable observation platforms for these studies given their capacity to operate under any weather conditions. In the future, the possible increase in the intensity and duration of the storms affecting the Western Mediterranean area (Gaertner et al., 2007, Romero and Emanuel, 2013, Gonzalez-Alemán et al. 2019) could lead to enhanced impacts of such storm-related upwelling events. While this study presents a first analysis over the last 9 years, it will be important to analyze these events in the longer term with a climate perspective when multi-decadal kilometer-scale reanalysis simulations become available in the study area.

Data availability

The model and observation products used in this study from both the Copernicus Marine Service and other sources are listed in Table 1.

Product ref. no.	Product ID & type	Data access	Documentation
1	Images from the Copernicus Sentinel-3; Satellite observations	Sentinel Hub services (EO Browser), sentinel-hub.com	Sentinel-3 Mission description: https://sentinels.copernicus.eu/web/sentinel/missions/sentinel-3 Data acquired by the Ocean and Land Colour Instrument (OLCI)
2	INSITU_MED_PHYBGCWAV_DISCRETE_MYNRT_013_035; In-situ observations	EU Copernicus Marine Service Product, https://marine.copernicus.eu/, 2021	PUM: https://catalogue.marine.copernicus.eu/documents/PUM/CMEMS-INS-PUM-013.pdf QUID: https://catalogue.marine.copernicus.eu/documents/QUID/CMEMS-INS-QUID-013-030-036.pdf
3	HARMONIE-AROME; Numerical weather prediction model	AEMET, Ministerio para la Transición Ecológica y el Reto Demográfico.	System description: https://www.aemet.es/en/noticias/2017/07/modelo_harmonie-arome (Bengtsson et al., 2017)
4	SOCIB-WMOP; Numerical ocean prediction model	SOCIB: http://thredds.socib.es/thredds/catalog/operational_models/oceanographical/hydrodynamics/wmop/catalog.html	Product description: http://socib.es/?seccion=modelling&facility=forecast_system_description (Juza et al., 2016; Mourre et al., 2018; Lasheras-Hernández and Mourre, 2018; Lasheras-Hernández et al., 2021)

5	MEDSEA_ANALYSIS_FORECAST_PHY_006_013; Numerical models	EU Copernicus Marine Service Product, https://marine.copernicus.eu/, 2021	PUM: https://catalogue.marine.copernicus.eu/documents/PUM/CMEMS-MED-PUM-006-013.pdf QUID: https://catalogue.marine.copernicus.eu/documents/QUID/CMEMS-MED-QUID-006-013.pdf
6	SST_MED_SST_L4_NRT_OBSERVATIONS_010_004; Satellite observations	EU Copernicus Marine Service Product, https://marine.copernicus.eu/, 2021	PUM: https://catalogue.marine.copernicus.eu/documents/PUM/CMEMS-SST-PUM-010-004-006-012-013.pdf QUID: https://catalogue.marine.copernicus.eu/documents/QUID/CMEMS-SST-QUID-010-004-006-012-013.pdf
7	SEALVEL_EUR_PHY_L3_NRT_OBSERVATIONS_008_059; Satellite observations	EU Copernicus Marine Service Product, https://marine.copernicus.eu/, 2021	PUM: http://marine.copernicus.eu/documents/PUM/CMEMS-SL-PUM-008-032-068.pdf QUID: http://marine.copernicus.eu/documents/QUID/CMEMS-SL-QUID-008-032-068.pdf
8	INSITU_GLO_PHY_UV_DISCRETE_NRT_013_048; In-situ observations	EU Copernicus Marine Service Product, https://marine.copernicus.eu/, 2021	PUM: https://catalogue.marine.copernicus.eu/documents/PUM/CMEMS-INS-PUM-013-048.pdf QUID: https://catalogue.marine.copernicus.eu/documents/QUID/CMEMS-INS-QUID-013-048.pdf
9	OCEANCOLOUR_MED_BGC_L3_NRT_009_141; Satellite observations	EU Copernicus Marine Service Product, https://marine.copernicus.eu/, 2021	PUM: https://catalogue.marine.copernicus.eu/documents/PUM/CMEMS-OC-PUM.pdf QUID: https://catalogue.marine.copernicus.eu/documents/QUID/CMEMS-OC-QUID-009-141to144-151to154.pdf

Table 1: Products from the Copernicus Marine Service and other complementary datasets used in this study, including the Product User Manual and quality information. For complementary datasets, the link to the product description, data access and scientific references are provided.

Acknowlegements

This study has been conducted using European Union´s Copernicus Marine Service Information. The results of this article have been obtained using also the HARMONIE-AROME atmospheric fields provided by the Spanish Meteorological Agency (AEMET, Ministerio para la Transición Ecológica y el Reto Demográfico). The authors are very grateful to AEMET for providing these fields. The authors also thank SOCIB and Puertos del Estado for collecting oceanic and atmospheric observations around the Balearic Islands and distributing them through both their institutional websites and Copernicus database.

Authors contribution

B.M., E.R., A.S., J.H.L., I.H.C., M.G.J. and N.Z. designed the study through interactive discussions in the framework of working team meetings. B.M. and E.R. created the figures. B.M. prepared the article with contributions from all coauthors. E.R. analyzed HF Radar and in-situ observations. P.L. provided expertise in the definition of upwelling indices. A.S. analysed the atmospheric fields and computed the Ekman transport. N.Z. and I.H.C. contributed to the analysis of ocean colour images. J.H.L. and M.G.J. analysed WMOP and CMEMS-MED model outputs. All authors have participated in the iterations and revision of the manuscript.

Competing interests

The authors declare that they have no conflict of interest.

References

Álvarez-Fanjul, E., Pérez Gómez, M., Alonso-Muñoyerr, M. de A., Jiménez, P. L., Sotillo, M. G., Lin-Ye, J., Lecocq, A., Serna, M. R. G. de la, Rubio, S. P., Clementi, E., Coppini, G., García-León, M., Muñoz, D. S., Rico, M. Y. L., Mestres, M., Molina, R., Tintoré, J., Mourre, B., Masina, S., Mosso, C., Reyes, E., and Santana, A.: Western Mediterranean record-breaking storm Gloria: An integrated assessment based on models and observations, In: von Schuckmann K. et al. (2022), Copernicus Ocean State Report, issue 6, Journal of Operational Oceanography, 15:sup1, 1-220, , 2022.

Amores, A., Marcos, M., Carrió, D. S., and Gómez-Pujol, L.: Coastal impacts of Storm Gloria (January 2020) over the north-western Mediterranean, Natural Hazards and Earth System Sciences, 20, 1955–1968, 2020.

Bakun, A.: Coastal upwelling indices, west coast of North America, 1946-71, 1973.

Bakun, A. and Agostini, V. N.: Seasonal patterns of wind-induced upwelling/downwelling in the Mediterranean Sea, Sci. Mar., 65(3), 243–257, 2001.

Bengtsson, L., Andrae, U., Aspelien, T., Batrak, Y., Calvo, J., Rooy, W. de, Gleeson, E., Hansen-Sass, B., Homleid, M., Hortal, M., and others: The HARMONIE–AROME model configuration in the ALADIN–HIRLAM NWP system, Monthly Weather Review, 145, 1919–1935, 2017.

Casella, E., Molcard, A., and Provenzale, A.: Mesoscale vortices in the Ligurian Sea and their effect on coastal upwelling processes, Journal of Marine Systems, 88, 12–19, 2011.

Clementi, E., Aydogdu, A., Goglio, A. C., Pistoia, J., Escudier, R., Drudi, M., Grandi, A., Mariani, A., Lyubartsev, V., Lecci, R., Cretí, S., Coppini, G., Masina, S., & Pinardi, N.: Mediterranean Sea Physical Analysis and Forecast (CMEMS MED-Currents, EAS6 system) (Version 1). Copernicus Monitoring Environment Marine Service (CMEMS), 2021.

Demarcq, H. and Faure, V.: Coastal upwelling and associated retention indices derived from satellite SST. Application to Octopus vulgaris recruitment, Oceanologica acta, 23, 391–408, 2000.

Dobricic, S. and Pinardi, N.: An oceanographic three-dimensional variational data assimilation scheme. Ocean Model. 22 (3-4), 89-105, 2008.

Gaertner, M. A., Jacob, D., Gil, V., Domiınguez, M., Padorno, E., Sánchez, E., and Castro, M.: Tropical cyclones over the Mediterranean Sea in climate change simulations, Geophysical Research Letters, 34, 2007.

García-León, M.: Coastal Risk Forecast System: Fostering Proactive Management at the Catalan Coast. Doctoral dissertation, Polytechnic University of Catalonia, Barcelona, 2018.

González-Alemán, J. J., Pascale, S., Gutierrez-Fernandez, J., Murakami, H., Gaertner, M. A., and Vecchi, G. A.: Potential increase in hazard from Mediterranean hurricane activity with global warming, Geophysical Research Letters, 46, 1754–1764, 2019.

Hernández-Lasheras, J. and Mourre, B.: Dense CTD survey versus glider fleet sampling: comparing data assimilation performance in a regional ocean model west of Sardinia, Ocean Science, 14, 1069–1084, 2018.

Hernández-Lasheras, J., Mourre, B., Orfila, A., Santana, A., Reyes, E., and Tintoré, J.: Evaluating high-frequency radar data assimilation impact in coastal ocean operational modelling, Ocean Science, 17, 1157–1175, 2021.

Jacox, M. G., Edwards, C. A., Hazen, E. L, and Bograd, S. J.: Coastal upwelling revisited: Ekman, Bakun, and improved upwelling indices for the U.S. west coast, Journal of Geophysical Research, 123(10), 7332-7350, 2018.

Juza, M., Mourre, B., Renault, L., Gómara, S., Sebastián, K., Lora, S., Beltran, J. P., Frontera, B., Garau, B., Troupin, C., and others: SOCIB operational ocean forecasting system and multi-platform validation in the Western Mediterranean Sea, Journal of Operational Oceanography, 9, s155–s166, 2016.

Kohut, J.T., Glenn, S.M., Paduan, J.D.: Inner-shelf response to tropical storm Floyd. J. Geophys. Res. 111, c09S91, 2006.

Lopez-García, M. J., Millot, C., Font, J., & Garcia-Ladona, E.: Surface circulation variability in the Balearic Basin. *Journal of Geophysical Research*, *99*(C2), 3285–3296, 1994.

Lorente, P., Piedracoba, S., Montero, P., Sotillo, M. G., Ruiz, M. I., and Álvarez-Fanjul, E.: Comparative Analysis of Summer Upwelling and Downwelling Events in NW Spain: A Model-Observations Approach, Remote Sensing, 12, 2762, 2020.

Lorente, P., Rubio, A., Reyes, E., Solabarrieta, L., Piedracoba, S., Álvarez-Fanjul, E., Tintoré, J and Mader, J.: High Frequency radar-derived coastal upwelling index. State of the Planet, Preprint,doi: 10.5194/sp-2022-5

Macías, D., Bruno, M., Echevarría, F., Vázquez, A., and García, C. M.: Meteorologically-induced mesoscale variability of the North-western Alboran Sea (southern Spain) and related biological patterns, Estuarine, Coastal and Shelf Science, 78, 250–266, 2008.

Marchesiello, P. and Estrade, P.: Upwelling limitation by onshore geostrophic flow, Journal of Marine Research, 68, 37–62, 2010.

Millot, C.: Wind induced upwellings in the Gulf of Lions, Oceanologica Acta, 2, 261–274, 1979.

Millot, C.: Some features of the Algerian Current, Journal of Geophysical Research: Oceans, 90, 7169–7176, 1985.

Mourre B., E. Aguiar, M. Juza, J. Hernandez-Lasheras, E. Reyes, E. Heslop, R. Escudier, E. Cutolo, S. Ruiz, E. Mason, A. Pascual and J. Tintoré: Assessment of high-resolution regional ocean prediction systems using multi-platform observations: illustrations in the Western Mediterranean Sea. In "New Frontiers in Operational Oceanography", E. Chassignet, A. Pascual, J. Tintoré and J. Verron, Eds, GODAE Ocean View, 663-694, doi: 10.17125/gov2018.ch24, 2018

Olita, A., Ribotti, A., Fazioli, L., Perilli, A., and Sorgente, R.: Surface circulation and upwelling in the Sardinia Sea: A numerical study, Continental Shelf Research, 71, 95–108, 2013.

Paduan, J.D., Rosenfeld, L.K.: Remotely sensed surface currents in Monterey Bay from shore-based HF radar (CODAR). J. Geophys. Res. 101, 20669–20686, 1996.

Rey, V., Dufresne, C., Fuda, J.-L., Mallarino, D., Missamou, T., Paugam, C., Rougier, G., and Taupier-Letage, I.: On the use of long-term observation of water level and temperature along the shore for a better understanding of the dynamics: example of Toulon area, France, Ocean Dynamics, 70, 913–933, 2020.

Romero, R. and Emanuel, K.: Medicane risk in a changing climate, Journal of Geophysical Research: Atmospheres, 118, 5992–6001, 2013.

Rossi, V., Feng, M., Pattiaratchi, C., Roughan, M., and Waite, A. M.: On the factors influencing the development of sporadic upwelling in the Leeuwin Current system, Journal of Geophysical Research: Oceans, 118, 3608–3621, 2013.

Salusti, E.: Satellite images of upwellings and cold filament dynamics as transient effects of violent air-sea interactions downstream from the island of Sardinia (western Mediterranean Sea), Journal of Geophysical Research: Oceans, 103, 3013–3031, 1998.

Sarhan, T., García-Lafuente, J., Vargas, M., Vargas, J. M., & Plaza, F.: Upwelling mechanisms in the northwestern Alboran Sea. Journal of Marine Systems, 23(4), 317–331, 2000.

Shchepetkin, A. F. and McWilliams, J. C.: The regional oceanic modeling system (ROMS): a split-explicit, free-surface, topography-following-coordinate oceanic model, Ocean modelling, 9, 347–404, 2005.

Sotillo, M. G., Mourre, B., Mestres, M., Lorente, P., Aznar, R., García-León, M., Liste, M., Santana, A., Espino, M., and Álvarez, E.: Evaluation of the operational CMEMS and coastal downstream ocean forecasting services during the storm Gloria (January 2020), Frontiers in Marine Science, 8, 644525, 2021.

Tintoré, J., Vizoso, G., Casas, B., E. Heslop et al.: SOCIB: the Balearic Islands Observing and Forecasting System responding to science, technology and society needs. Mar. Tech. Soc. J. 47:17, 2013.

Volpe, G., Colella, S., Brando, V. E., Forneris, V., Padula, F. L., Cicco, A. D., Sammartino, M., Bracaglia, M., Artuso, F., and Santoleri, R.: Mediterranean ocean colour Level 3 operational multi-sensor processing, Ocean Science, 15, 127–146, 2019.